J|A|C|S
ARTICLES

Published on Web 10/27/2009

"Hairy" Poly(3-hexylthiophene) Particles Prepared via Surface-Initiated Kumada Catalyst-Transfer Polycondensation

Volodymyr Senkovskyy,[†] Roman Tkachov,[†] Tetyana Beryozkina,[†] Hartmut Komber,[†] Ulrich Oertel,[†] Marta Horecha,[†] Vera Bocharova,[†] Manfred Stamm,[†] Suren A. Gevorgyan,[‡] Frederik C. Krebs,[‡] and Anton Kiriy*,[†]

Leibniz-Institut für Polymerforschung Dresden e.V., Hohe Straße 6, 01069 Dresden, Germany, and Risø National Laboratory for Sustainable Energy, Technical University of Denmark, Frederiksborgvej 399, DK-4000 Roskilde, Denmark

Received June 15, 2009; E-mail: kiriy@ipfdd.de; senkovskyy@ipfdd.de

Abstract: Herein, we present a new paradigm in the engineering of nanostructured hybrids between conjugated polymer and inorganic materials via a chain-growth surface-initiated Kumada catalyst-transfer polycondensation (SI-KCTP) from particles. Poly(3-hexylthiophene), P3HT, a benchmark material for organic electronics, was selectively grown by SI-KCTP from (nano)particles bearing surface-immobilized Ni catalysts supported by bidentate phosphorus ligands, that resulted in hairy (nano)particles with end-tethered P3HT chains. Densely grafted P3HT chains exhibit strongly altered optical properties compared to the untethered counterparts (red shift and vibronic fine structure in absorption and fluorescence spectra), as a result of efficient planarization and chain-aggregation. These effects are observed in solvents that are normally recognized as good solvents for P3HT (e.g., tetrahydrofurane). We attribute this to strong interchain interactions within densely grafted P3HT chains, which can be tuned by changing the surface curvature (or size) of the supporting particle. The hairy P3HT nanoparticles were successfully applied in bulk heterojunction solar cells.

Introduction

It is well-established that performances of thin-film devices based on π-conjugated polymers (CPs), for example, solar cells, field-effect transistors, and light-emitting diodes, are strongly dependent on the organization of the polymer molecules and their interactions with other constituents in the multicomponent devices.[1] Further progress of organic electronics will require a development of new CPs having not only improved optoelectronic characteristics, but also guidable self-assembly properties.[1] In general, self-assembly is a powerful and cost-efficient approach in the fabrication of complex nanostructured materials. However, it works more predictably in the case of relatively simple, shape-persistent, chemically well-defined building blocks, such as conjugated oligomers or macrocycles.[2] CPs are usually more flexible, larger, and less defined in terms of molecular weight distribution and chemical structure when comparing to their small-molecule counterparts and they exhibit very complex self-assembly behavior. In addition, films of CPs formed from solution rarely give optimally organized structures as prepared, and this can pose problems when they must be delicately organized together with other components, such as in bulk heterojunction solar cells.[1]

We assumed that self-assembly of complex multicomponent functional structures would be subject to a higher degree of control, if relatively large (but still nanoscale), three-dimensional, shape-persistent, and covalently preorganized building blocks were used. We supposed that "hairy" particles, nanoscale objects in which polymer chains are attached by their end points to a particle core and stretched away from it to form spherical brushes, would be such an interesting alternative to conventional linear CPs. In addition, conjugated polyelectrolytes (charged CPs)[3] densely grafted to microsperes would be an attractive approach to sensor applications. The "grafting-to" approach based on a coupling of end-functionalized polymers with complementarily terminated surfaces usually provides rather low grafting densities.[4] This method that has been widely employed

[†] Leibniz-Institut für Polymerforschung Dresden e.V.
[‡] Technical University of Denmark.

(1) (a) Hoppe, H.; Sariciftci, N. S. *J. Mater. Chem.* **2006**, *16*, 45–61. (b) Thompson, B. C.; Fréchet, J. M. J. *Angew. Chem., Int. Ed.* **2008**, *47*, 58–77. (c) Kroon, R.; Lenes, M.; Hummelen, J. C.; Blom, P. W. M.; De Boer, B. *Polym. Rev.* **2008**, *48*, 531–582. (d) Kiriy, N.; Bocharova, V.; Kiriy, A.; Stamm, M.; Krebs, F. C.; Adler, H.-J. *Chem. Mater.* **2004**, *16*, 4765–4771. (e) Kiriy, N.; Kiriy, A.; Bocharova, V.; Stamm, M.; Richter, S.; Plötner, M.; Fischer, W.-J.; Krebs, F. C.; Senkovska, I.; Adler, H.-J. *Chem. Mater.* **2004**, *16*, 4757–4764. (f) Bundgaard, E.; Krebs, F. C. *Sol. Energy Mater. Sol. Cells* **2007**, *91*, 954–985. (g) Boucle, J.; Ravirajan, P.; Nelson, J. *J. Mater. Chem.* **2007**, *17*, 3141–3153. (h) Peet, J.; Senatore, M. L.; Heeger, A. J.; Bazan, G. C. *Adv. Mater.* **2009**, *21*, 1521–1527.

(2) (a) Cavallini, M.; Stoliar, P.; Moulin, J. F.; Surin, M.; Leclere, P.; Lazzaroni, R.; Breiby, D. W.; Andreasen, J. W.; Nielsen, M. M.; Sonar, P.; Grimsdale, A. C.; Müllen, K.; Biscarini, F. *Nano Lett.* **2005**, *5*, 2422–2425. (b) Kiriy, N.; Bocharova, V.; Kiriy, A.; Stamm, M.; Krebs, F. C.; Adler, H.-J. *Chem. Mater.* **2004**, *16*, 4765–4771.

(3) (a) McQuade, D. T.; Pullen, A. E.; Swager, T. M. *Chem. Rev.* **2000**, *100*, 2537–74. (b) Ho, H. A.; Dore, K.; Boissinot, M.; Bergeron, M. G.; Tanguay, R. M.; Boudreau, D.; Leclerc, M. *J. Am. Chem. Soc.* **2005**, *127*, 12673–76. (c) McRae, R. L.; Phillips, R. L.; Kim, I.-B.; Bunz, U. H. F.; Fahrni, C. J. *J. Am. Chem. Soc.* **2008**, *130*, 7851–7853. (d) Ogawa, K.; Chemburu, S.; Lopez, G. P.; Whitten, D. G.; Schanze, K. S. *Langmuir* **2007**, *23*, 4541–4548.

(4) Brittain, W. J.; Minko, S. *J. Polym. Sci., Part A: Polym. Chem.* **2007**, *45*, 3505–3512.

Scheme 1. Different Ways To Initiate Kumada Polycondensation into Polyalkylthiophenes

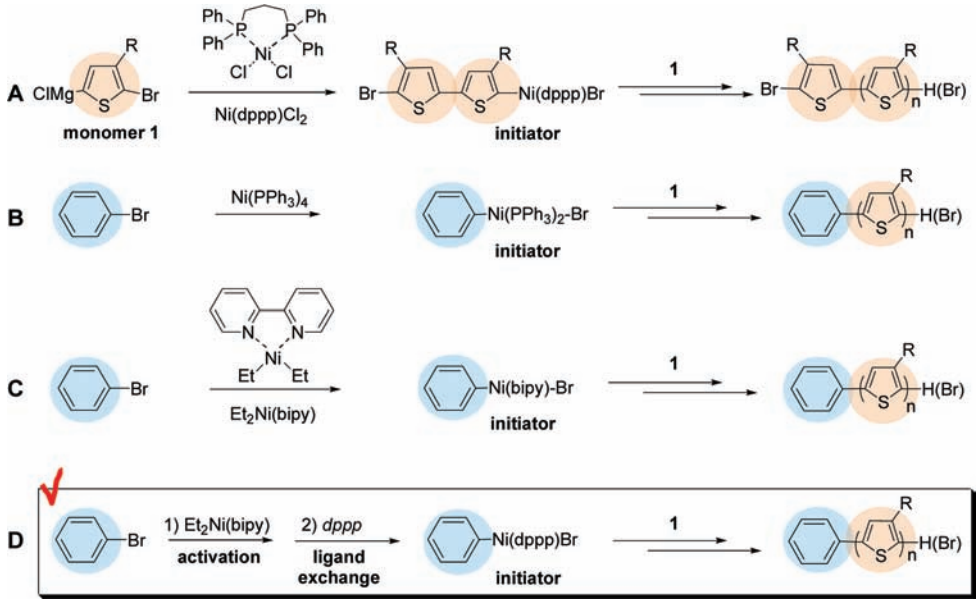

in the modification of particles by nonconjugated polymers has also been exemplified in the grafting of conjugated polymers, for example, by attachment of thiol end-functionalized polyacetylene to gold nanoparticles[5a] or amino-functionalized P3HT to quantum dots.[5b] There are few examples in the literature describing the "reactive-grafting-onto" approach whereby growing CP polymer chains are grafted onto properly functionalized reactive surfaces.[5c] Following this strategy, Schanze et al. performed grafting of polyacetylene that resulted in polymer brushes that were limited to 12 nm thicknesses.[3d]

Surface-initiated polymerization, or the "grafting-from" approach,[6] the method of growing polymer chains selectively from functionalized particles via one-by-one addition of monomers to surface-immobilized initiators, is one of the most powerful synthetic approaches to hairy particles with variable composition and a tunable grafting density. However, to the best of our knowledge, this approach has never been successfully applied for the grafting of conjugated polymers from particles because of a step-growth character of most of synthetic routes to CPs.[7] A few years ago, the groups of McCullough[8] and Yokozawa[9] made the important discovery that Kumada polycondensation into regioregular poly(3-hexythiophene), P3HT, follows a chain-growth mechanism and, therefore, it might become a suitable process for surface-initiated polymerizations. Unfortunately, in its "classical" form, the Kumada polycondensation does not allow surface tethering due to the requirement for a monomer−monomer initiation stage (Scheme 1A). Recently we found a method to prepare a series of Ar-$(PPh_3)_2$-X initiators via an oxidative addition of Ar-X to $Ni(PPh_3)_4$. These initiators were found to efficiently initiate the polymerization of P3HT[10] (Scheme 1B). We also developed surface-initiated Kumada catalyst-transfer polycondensation (SI-KCTP) of P3HT from properly modified planar surfaces.[10−12] However, a direct comparison of the Ph-Ni$(PPh_3)_2$-Br and Ni(dppp)Cl_2 (dppp = $Ph_2P(CH_2)_3PPh_2$) catalysts reveals that the former complex exhibits much poorer polymerization performance than the latter one, as a result of extensive chain-termination and reinitiation reactions. Another problem of the developed method is associated with extensive homocoupling side reactions that take place during the oxidative addition of $Ni(PPh_3)_4$ to aryl halides, especially in the case of *para*-substituted aryl halides or if a number of such groups are located closely to each other. In the present work we found that the latter obstacle almost completely prevents the grafting of P3HT from particles and only ungrafted P3HT is formed instead. Herein we describe a new route to a library of highly efficient surface-immobilized Ni initiators supported by nitrogen- and phosphorus-based *bidentate* ligands that allows for the initiation of polymerization into regioregular P3HT with controlled molecular weight and narrow dispersity. This novel initiating method was successfully applied in selective grafting of regioregular P3HT from submicrometer and nonoscale organosilica particles. Optical and photovoltaic properties of hairy P3HT nonoparticles are also presented.

Results and Discussion

Externally Initiated KCTP. 2,2′-Bipyridyl (bipy)-Supported Initiators. Widely used in Yamamoto polycondensation

(5) (a) Nakashima, H.; Furukawa, K.; Ajito, K.; Kashimura, Y.; Torimitsu, K. *Langmuir* **2005**, *21*, 511–515. (b) Liu, J.; Tanaka, T.; Sivula, K.; Alivisatos, A. P.; Frechet, J. M. J. *J. Am. Chem. Soc.* **2004**, *126*, 6550–52. (c) Odoi, M. Y.; Hammer, N. I.; Sill, K.; Emrick, T.; Barnes, M. D. *J. Am. Chem. Soc.* **2006**, *128*, 3506–3512.

(6) Edmondson, S.; Osborne, V. L.; Huck, W. T. S. *Chem. Soc. Rev.* **2004**, *33*, 14–22.

(7) Iovu, M. C.; Sheina, E. E.; Gil, R. R.; McCullough, R. D. *Macromolecules* **2005**, *38*, 8649–8656.

(8) Miyakoshi, R.; Yokoyama, A.; Yokozawa, T. *J. Am. Chem. Soc.* **2005**, *127*, 17542–17547.

(9) (a) Schlüter, D. *J. Polym. Sci., Part A: Polym. Chem.* **2001**, *39*, 1533. (b) Yamamoto, T. *Macromol. Rapid Commun.* **2002**, *23*, 583.

(10) (a) Senkovskyy, V.; Khanduyeva, N.; Komber, H.; Oertel, U.; Stamm, M.; Kuckling, D.; Kiriy, A. *J. Am. Chem. Soc.* **2007**, *129*, 6626–6632. (b) Khanduyeva, N.; Beryozkina, T.; Senkovskyy, V. N.; Simon, F.; Nitschke, M.; Stamm, M.; Kiriy, A. *Macromolecules* **2008**, *41*, 7383–7389.

(11) (a) Beryozkina, T.; Senkovskyy, V.; Kaul, E.; Kiriy, A. *Macromolecules* **2008**, *41*, 7817–7823. (b) Khanduyeva, N.; Senkovskyy, V.; Beryozkina, T.; Horecha, M.; Stamm, M.; Uhrich, C.; Riede, M.; Leo, K.; Kiriy, A. *J. Am. Chem. Soc.* **2009**, *131*, 153–161. (c) Kiriy, A.; Senkovskyy, V.; Stamm, M. EU patent application number EP 09 005 837.1, filed April 27, 2009.

(12) Surface-initiated Suzuki polycondensation from planar surfaces was also reported: Beryozkina, T.; Boyko, K.; Khanduyeva, N.; Senkovskyy, V.; Horecha, M.; Oertel, U.; Simon, F.; Stamm, M.; Kiriy, A. *Angew. Chem., Int. Ed.* **2009**, *48*, 2695–2698.

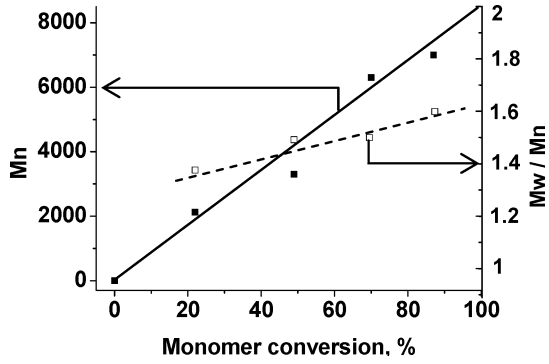

Figure 1. Number-average molecular weight (M_n), calculated molecular weight (M_{ncal}, dotted line), and dispersity (M_w/M_n) as a function of the monomer **1** conversion for the polycondensation initiated by Ph-Ni(bipy)-Br at 50/1 feed ratio. M_{ncal} is calculated by assuming that the polymerization follows a "living" mechanism.

reactions are Ni complexes supported by bipy[9b] that attracted our attention as a potentially viable alternative to phosphorus-containing catalysts.[13] To establish the applicability of bipy as the supporting ligand in KCTP, the polymerization of 2-bromo-5-chloromagnesio-3-hexylthiophene (**1**) was performed in the presence of Ni(bipy)Cl_2 in freshly distilled (under sodium benzophenone ketyl) THF.[14] The polymerization led to highly regioregular head-to-tail (HT) P3HT in a broad range of polymerization temperatures (up to 50 °C). The reaction was found to involve a chain-growth polymerization mechanism, following a gradual growth of the number-average molecular weight (M_n) with polymerization time (Figure S2, SI). Moderate dispersities, $D = M_w/M_n$ (M_w is the weight-average molecular weight and M_n is the number average molecular weight), in the 1.4−1.6 range were achievable when the polycondensation was conducted in freshly distilled THF (SI, Figures S2−S4).

An attractive feature of Ni(bipy)-based chemistry is that various Ar-Ni(bipy)-Br compounds can be obtained in pure form and in high yield by the reaction of diethylbipyridylnickel, Et_2Ni(bipy), with aryl halides.[15,16] A model initiator Ph-Ni(bipy)-Br was prepared from Et_2Ni(bipy), and bromobenzene as a model aryl halide (Scheme 1C). The course of the reaction could be followed easily by a change of the color of the reaction mixture from green (before addition of Ph-Br) to red at the end of the reaction. The reaction course of Ph-Br with Et_2Ni(bipy) was examined using ^{1}H NMR by performing the reaction directly in the NMR tube. Fortunately, the reaction proceeds cleanly and no other products besides Ph-Ni(bipy)-Br were detected in this experiment. As in the case of Ni(bipy)Cl_2, Ph-Ni(bipy)-Br initiated polycondensation of **1** conducted at room temperature in freshly distilled THF affords regioregular HT P3HT and allows moderate control over the molecular weight, MW, and dispersities of about 1.4−1.6 (Figure 1). Careful inspection of the ^{1}H NMR spectrum allows for the identification of the end groups of the P3HT product, as shown in Figure S3. Integration of the spectra shows that the H- and Br-termini (signals at 6.95−6.82 ppm) are present in an excess compared to the Ph-termination (7.59, 7.38, 7.29, Figure S3). This result suggests that besides the "ideal" Ph/H chain-growth product, the reaction mixture also contains rather significant amounts of H/Br-terminated P3HT (>35%), formed presumably due to a chain-termination and reinitiation processes. A comparison of these results with literature data for Ni(dppp)Cl_2-catalyzed polymerizations[7,8] allows for the conclusion that the latter complex significantly outperforms other catalysts for Kumada polycondensation reactions, and therefore, initiators supported by bidentate phosphorus ligands remained an attractive target.

Initiators Supported by Bidentate Phosphorus Ligands. A ligand-exchange strategy was applied to prepare desired Ph-Ni(dppp)-Br and Ph-Ni(dppe)-Br (dppe = $Ph_2P(CH_2)_2PPh_2$) initiators from Ph-Ni(bipy)-Br via its reaction with dppp or dppe ligands to replace bipy by the phosphorus containing ligands (Scheme 1D). The course of the two-step transformation can be monitored by changes of the color of the reaction mixture. Thus, the addition of Et_2Nibipy to Ph-Br is accompanied by a color change from the green to the reddish-brown; the subsequent addition of dppp (or dppe) resulted in a color change of the reaction mixture to orange-yellow. Structures of the formed Ph-Ni(dppp)-Br and Ph-Ni(dppe)-Br complexes were unambiguously proven by ^{1}H, ^{13}C, and ^{31}P NMR analysis data (Figure S4).

The observed nonequivalence of the phosphorus sites is in accordance with literature data for Ph-Ni(dppe)-Cl.[17] The course of both reactions (Ph-Br with Et_2Ni(bipy) and Ph-Ni(bipy)-Br with dppe) was monitored using ^{1}H NMR and ^{31}P NMR by performing the reaction directly in the NMR tube. Fortunately, no side products were detected upon the two-step transformation (Scheme 1D).

An attractive feature of the ligand-exchange method is its universal nature. By using our approach, a library of Ar-Ni(L_2)-X initiators with a tunable reactivity can be prepared within the same synthetic protocol. Variation of the nature of the supporting ligands would be a powerful tool in optimization of the polymerization performance. It has earlier been demonstrated that dppp as supporting ligand significantly outperforms dppe in the preparation of P3ATs,[7,8] whereas dppe is better suited for the preparation of polypyrroles, polyphenylenes,[18] and polythiophenes with oxyethylene side groups.[19]

We found that room temperature polycondensation of **1** initiated by Ph-Ni(dppp)-Br affords regioregular head-to-tail P3HT with a good control of the MW, as seen from the near linear dependence of the number-average molecular weight (M_n) on monomer conversion (Figure 2). The polymerization is less controlled at polymerization degrees (DP) higher than 100 due to limited and MW-dependent solubility of P3HT. High MW P3HT, however, can be obtained performing the polymerization at higher temperatures or by use of other solvents.[20] Importantly, polydispersities of moderate MW P3HT obtained by this method falls into the same range as those achievable by use of Ni(dppp)Cl_2 as catalyst, for example, in the 1.1−1.2 range.[7,8]

(13) Structurally similar Ni-diimine complexes were recently applied as catalysts in the preparation of regioregular P3HT: Sheina, E. E.; Iovu, M. C.; McCullough, R. D. *Polym. Prepr.* **2005**, *46* (2), 1070.
(14) Ni(bipy)-catalyzed polymerizations are sensitive to the solvent (i.e., THF) quality, therefore, freshly distilled THF must be used for obtaining of P3HT with monomodal MW distribution; for further details see SI, Figures S2−S4.
(15) Kiso, Y.; Yamamoto, K.; Tamao, K.; Kumada, M. *J. Am. Chem. Soc.* **1972**, *94*, 4374–4376.
(16) Wilke, G.; Herrmann, G. *Angew. Chem., Int. Ed.* **1966**, *5*, 581–582.
(17) Yamamoto, T.; Kohara, T.; Osakada, K. *Bull. Chem. Soc. Jpn.* **1983**, *56*, 2147–2153.
(18) Miyakoshi, R.; Shimono, K.; Yokoyama, A.; Yokozawa, T. *J. Am. Chem. Soc.* **2006**, *128*, 16012–16013.
(19) Adachi, I.; Miyakoshi, R.; Yokoyama, A.; Yokozawa, T. *Macromolecules* **2006**, *39*, 7793–7795. Yokoyama, A.; Kato, A.; Miyakoshi., R.; Yokozawa, T. *Macromolecules* **2008**, *41*, 7271–7273.
(20) Hiorns, R. C.; de Bettignies, R.; Leroy, J.; Bailly, S.; Firon, M.; Sentein, C.; Khoukh, A.; Preud'homme, H.; Dagron-Lartigau, C. *Adv. Funct. Mater.* **2006**, *16*, 2263–2273.

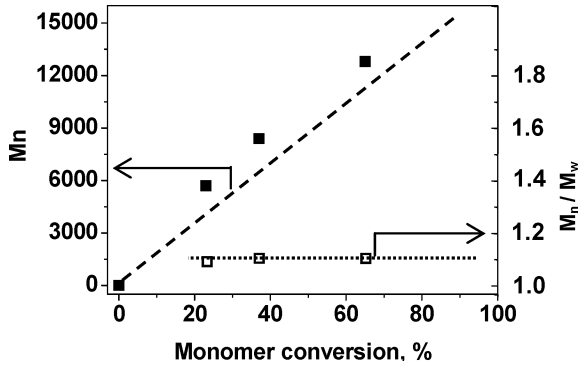

Figure 2. Number-average molecular weight (M_n), calculated molecular weight (M_{ncal}, dotted line), and dispersity (M_w/M_n) as a function of the monomer **1** conversion for the polycondensation initiated by Ph-Ni(dppp)-Br at 100/1 feed ratio. M_{ncal} is calculated by assuming that the polymerization follows a "living" mechanism.

Careful inspection of the ^{1}H NMR spectrum allows for the identification of the end groups of the P3HT product, as shown in Figure S5 in the Supporting Information. Integration of the spectrum reveals that the only Ph/H-terminated P3HT is formed reflecting that the termination and reinitiation side-reactions are negligible. We found that Ph-Ni(dppe)-Br also induces the chain-growth polycondensation of **1**, resulting in Ph-terminated P3HT (Figure S6) with somewhat higher dispersities of ~1.3.

Supporting Particles. Submicrometer organosilica spheres were prepared and used in this work as convenient model particles for development of the SI-KCTP since (i) near monodisperse silica spheres of controlled size and surface chemistry are easily available by a Stöber method;[21a] (ii) relatively large size and high density of the particles facilitate separation of surface-grafted materials from ungrafted ones by a simple centrifugation procedure; (iii) silica particles can be selectively etched under mild conditions without destruction of attached polymers, and therefore, the grafted polymers can be released from the support for further analysis; and (iv) submicrometer particles possess enough surface area to enable the collection of sufficient quantities of degrafted polymers for analysis from a single conventional laboratory-scale experiment. This is in stark contrast to the case when planar surfaces are used as supports.

Monodisperse, ~460 nm in the diameter, silica-core organosilica-shell particles were prepared by a modified Stöber method[21b] via sequential sol−gel hydrolysis of tetramethyl orthosilicates (TMOS) and [2-(4-bromo-phenyl)-ethyl]-triethoxisilane (**2**) under controlled conditions (Scheme 2A). Organosilane **2** obtained by a standard hydrosililation of 4-bromostyrene by triethoxisilane in the presence of chloroplatinic acid catalyst, was used in the particles synthesis to introduce bromophenyl surface-functionality which is necessary for the immobilization of Ni catalysts. According to thermogravimetric analysis, TGA (Figure 3c, black curve), the resulting particles contain ~10% of organosilane residues.

Grafting from Organosilica Particles. Attempting SI-KCTP with PPh_3-Supported Initiators. An approach based on the use of a $Ni(PPh_3)_4$ initiator served as the starting point in our trials to grow P3HT from the 460 nm organosilica particles. To immobilize the Ni catalyst, suspensions of the organosilica particles in anhydrous and degassed THF or toluene were mixed with $Ni(PPh_3)_4$ solutions in the same solvents under argon at room temperature for a period from 2 to 24 h. Prior to the polymerization, thus-treated particles were either purified from unreacted $Ni(PPh_3)_4$ and byproduct by repeated redispersion/centrifugation cycles or used in the grafting experiments without purification. Grafting of P3HT was attempted by the addition of **1** followed by stirring overnight. After quenching of the polymerization mixture with 5 N HCl, the particles were carefully purified from any ungrafted materials by redispersion in various solvents followed by centrifugation. Virtually no conversion of the monomer was observed in experiments that used particles purified after the catalyst immobilization step. When this purification step was omitted, all of the monomer was consumed in the formation of ungrafted P3HT. In all experiments the recovered particles were almost colorless, which is a good indication that the grafting process has failed. This was confirmed when analyzing using TGA showed no grafting of P3HT to the particles. These results suggested that the failure of the polymer grafting originated from unsuccessful immobilization of the $Ni(PPh_3)_4$ catalyst and from early chain terminations.

Attempting SI-KCTP with bipy-Suppported Initiators. To develop |-Si-$(CH_2)_2$-C_6H_4-Ni(bipy)-Br initiating sites, the 460 nm organosilica particles were treated with $Et_2Ni(bipy)$ followed by careful purification from physiosorbed Ni compounds by several centrifugation/redispersion cycles using anhydrous and degassed THF in an argon atmosphere. To perform SI-KCTP, monomer **1** was injected into the dispersion of the activated particles and the mixture was stirred at room temperature for several hours. After quenching of the reaction with 5 N HCl, the resulting particles were carefully separated from any ungrafted polymers, catalyst, and byproducts by several centrifugation/redispersion cycles using water, methanol, and hot chloroform. Unfortunately, only a marginal grafting of P3HT onto the particles was observed and a large amount of monomer **1** was consumed in the formation of ungrafted P3HT. Although the resulting particles exhibited a color inherent to low MW P3HTs (i.e., yellow in chloroform, reddish-brown in a solid state), the amount of the grafted material was so low that a quantitative evaluation of it using degrafting experiments or TGA was unsuccessful.

High-Performance SI-KCTP with dppp- and dppe-Supported Initiators. To develop |-Si-$(CH_2)_2$-C_6H_4-Ni(dppp)-Br or |-Si-$(CH_2)_2$-C_6H_4-Ni(dppe)-Br initiating sites, the organosilica particles were treated with $Et_2Ni(bipy)$ followed by the addition of an excess of the dppp or dppe ligands (Scheme 2B). Prior to the grafting it was found necessary to carefully purify the particles from physiosorbed Ni compounds by several centrifugation/redispersion cycles using anhydrous and degassed THF and CH_2Cl_2 in an argon atmosphere. It is important to note that CH_2Cl_2 is much better solvent than THF for many Ni complexes and thus its use in the purification procedure is desired. However, CH_2Cl_2 treatments can be only applied to relatively stable Ar-Ni(dppp)-Br and Ar-Ni(dppe)-Br complexes and not in the case of easily decomposable Ar-Ni(bipy)-Br.

To perform SI-KCTP, monomer **1** was added into the dispersion of the activated particles, and the polymerizations were performed at room temperature. After the polymerization, the resulting composite particles, further designated as μ-P3HT particles, were carefully separated from any ungrafted polymers, catalyst, and byproducts. A typical purification procedure included several centrifugation/redispersion cycles using the following solvents and additives in the following sequence: 5 N HCl, water, aqueous hydrosine hydrate, water, methanol, and hot chloroform. The latter centrifugation/redispersion cycles were repeated until the supernatant solutions after the centrifu-

Scheme 2. Preparation of Organosilica Particles via a Modified Stöber Method; Immobilization of Ni-Catalyst and SI-KCTP of **1** from the Modified Particles To Form Hairy P3HT Particles

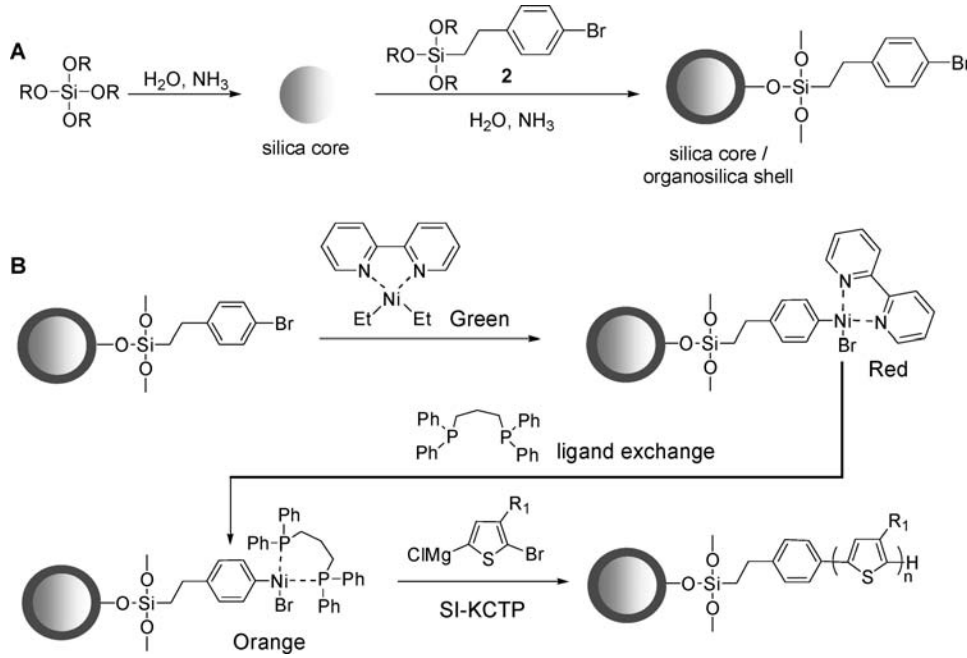

gation procedure remained colorless. Typically, much less than 10% of unbound P3HT was formed in SI-KCTP supported by dppp and dppe ligands reflecting a good selectivity of the grafting-from the nanoparticles.

A significantly lower selectivity of the bipy-based SI-KCTP compared to the case of dppp- and dppe-based SI-KCTPs may not solely be explained by a difference in the polymerization performances for the parent Ph-Ni(bipy)-Br and Ph-Ni(dppp)-Br initiators (compare Figures 1 and 2). Most likely, problems with bipy-based SI-KCTP originate from a relatively low stability of the |-Si-$(CH_2)_2$-C_6H_4-Ni(bipy)-Br initiator sites on the particle surface that easily decompose forming poorly soluble compounds. The later Ni compounds cannot be efficiently removed from the particles (they are not soluble in THF, whereas CH_2Cl_2 cannot be applied since this decomposes the remaining |-Si-$(CH_2)_2$-C_6H_4-Ni(bipy)-Br sites), and after the addition of the monomer **1**, the polymerization proceeds predominantly in the bulk solution. Luckily, the Ar-Ni(dppp)-Br and Ar-Ni(dppe)-Br complexes are stable in many solvents and in the presence of water and oxygen. Thus, to cleanly perform the SI-KCTP process, the dppp or dppe ligands must be added as early as possible to the particles treated with Et_2Ni(bipy) to stabilize the initiating sites. Even if some quantities of Ni-containing byproduct were formed upon the two-step activation, they can be easily washed away by "strong" solvents, like CH_2Cl_2.

The prepared hairy particles having a 460 nm organosilica core and P3HT shells (μ-P3HT particles) were extensively characterized. SEM measurements reveal that SI-KCTP induces a significant increase of the particles surface roughness and increase of their diameter from 460 nm for unmodified particles (Figure 3a) up to 498 nm for the μ-P3HT particles (Figure 3b). According to TGA (Figure 3c), the μ-P3HT particles loose ~13% of their weight in the temperature interval from 450 to 550 °C in an oxygen atmosphere that is a typical decomposition behavior of P3ATs. For the given particle size and densities of the components, the observed weight loss corresponds to the thicknesses of the P3HT shell, h, of about 20 nm (Table 1).

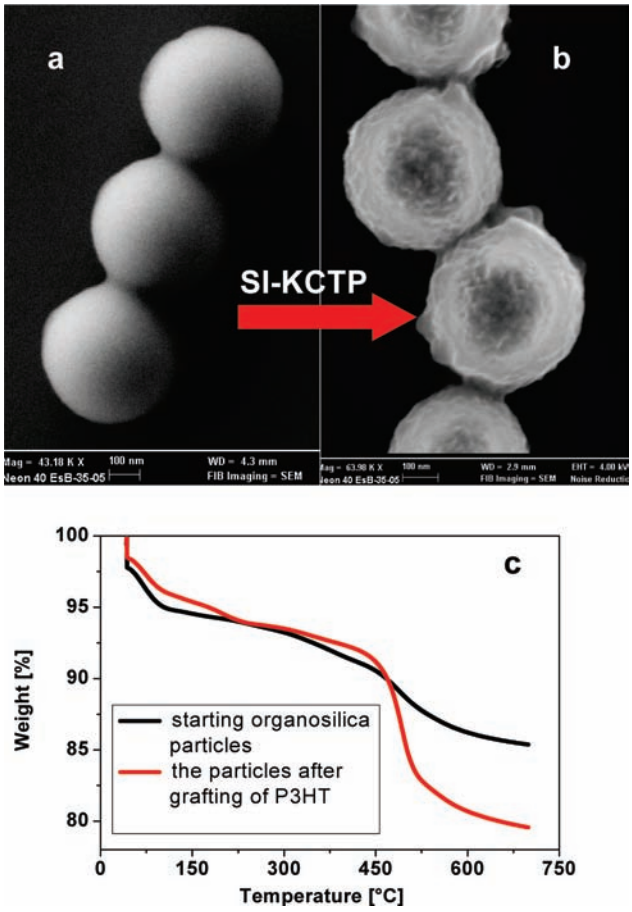

Figure 3. SEM images of the 460 nm organosilica particles before (a) and after (b) modification with P3HT via SI-KCTP of **1**. (c) TGA traces of the particles: starting organosilica particles, black curve; the particles with P3HT shell, red curve.

Table 1. Characterization Data for the Hairy Particles Obtained by the dppp-Supported SI-KCTP

sample name	core diameter, nm	shell thickness, nm	DP of grafts	TGA data, weight loss at 450−550 °C, %	UV−vis, nm	emission in THF, nm
μ-P3HT	460	2.0[a]	~250[b]	1.3	518, 555, 620[c]	573, 670, 730[c]
μ-P3DDT	460	2.5[a]	ND	1.7	465, 533, 580, 630[c]	551, 601, 665
nano-P3HT	4	6.5[d]	24[d,e]	95.7	450[c] (517, 550, 598)[f]	560

[a] Calculated from TGA data. [b] Calculated from GPC data for the degrafted polymer. [c] Measured in THF. [d] DLS data. [e] Calculated from ^{1}H NMR data; ND, not determined. [f] Measured in dry state.

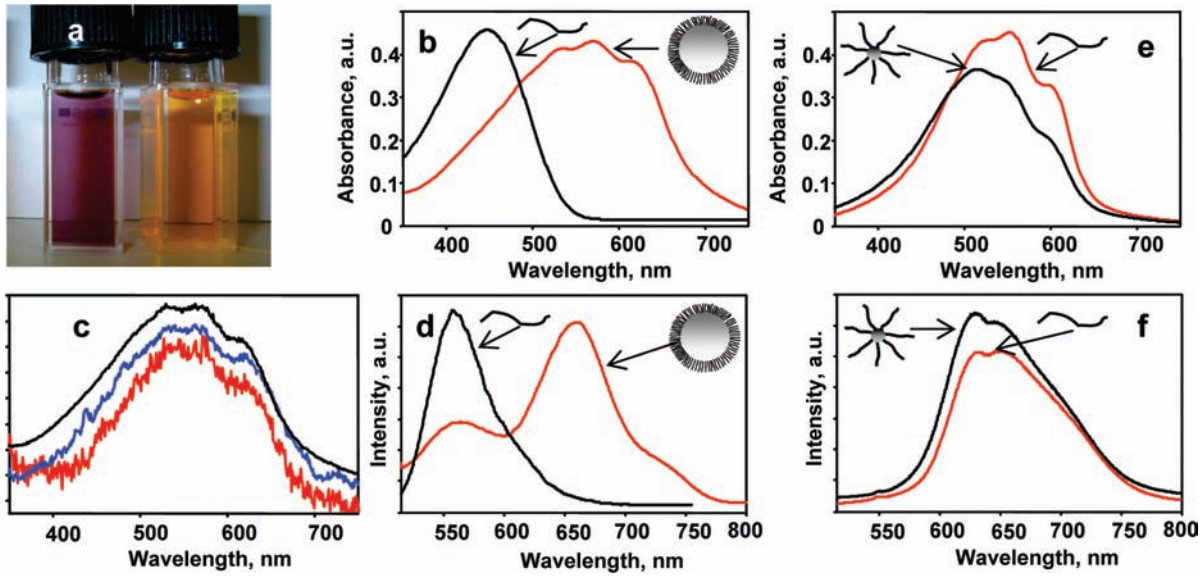

Figure 4. (a) Photograph of the dispersion of the μ-P3HT particles in THF (left-hand cuvette) and of the solution in THF of P3HT detached from the μ-P3HT particles (right-hand cuvette). UV−vis (b,c) and fluorescence (d) spectra of the dispersion of the μ-P3HT particles in THF (red lines in b and d) and of the solution in THF of P3HT detached from the μ-P3HT particles (black lines in b and d). (c) Concentration-independent normalized UV−vis spectra of the dispersions of the μ-P3HT particles in THF: 0.1 mg/mL (black curve); 0.02 mg/mL (blue curve); 0.004 mg/mL (red curve). UV−vis (e) and fluorescence (f) spectra of thermally annealed (150 °C, 5 min) films of the *nano*-P3HT particles (black lines in e and f) and of linear P3HT with M_n = 8000 and M_w = 13300 g/mol (red lines in e and f).

For analytical purposes, grafted P3HT chains were detached from the silica core of the μ-P3HT particles by dissolution of the latter in an aqueous hydrofluoric acid (HF). The mass fraction of the released polymer relative to the mass of the sample before the HF-treatment was found to be ~11% that agrees well with the TGA data. NMR analysis reveals a high head-to-tail regioregularity of P3HT (Figure S7). The detached P3HT exhibits a bimodal GPC trace with M_n = 43000 g/mol and M_w = 112000 g/mol (Figure S8). Most likely, the bimodal MW distribution originates from incomplete cleavage of Si−O and Si−C bonds caused by a poor compatibility of hydrophobic P3HT and aqueous HF. This assumption follows from a substantially increased fraction of the lower MW P3HT, when the HF-treatment was performed twice. Thus, we suggest that the lower MW peak corresponds to individual P3HT grafts with a per-graft DP of ~250, whereas the higher MW peak relates to incompletely disintegrated fragments of the particles, that is, to aggregates with a few-chains of P3HT.[22]

From these data, a reduced tethered density, Σ, an important parameter showing to what extent the conformation of the tethered polymer deviates from its unperturbed conformation in solution, can be estimated.[4] Because of the rather low surface curvature of the supporting particle (the core diameter is 460 nm and the contour length of the grafted chains is less than 100 nm), the following equation for planar brushes was applied: $\Sigma = \sigma\pi R_g^2$, where σ is a grafting density determined as the number of grafted chains per surface unit and R_g is the radius of gyration of P3HT with M_w = 42000 g/mol.[4] The calculated value for the reduced tethered density, Σ, based on the experimental data for the grafting density of P3HT chains (0.28 chains/nm^2) gives a value of 148 which correspond to a "true brush" regime of quite densely grafted and strongly stretched chains (Figures S9 and S10). As a result of the high grafting density, the hairy P3HT particles display much higher colloidal stability than the parent unmodified particles.

It is also interesting to note that the photophysical properties of the chains tethered to the μ-P3HT particles differ significantly from those for P3HT detached from the particles. Thus, we found that P3HT degrafted from the 460 nm particles exhibit optical properties usual for P3HT (orange color of the THF solution with λ_{max} = 450 nm and λ_{em} = 560 nm, Figure 4b,d, black lines). In sharp contrast, the dispersion of the μ-P3HT in THF that has a violet color and strongly red-shifted and structured absorption and fluorescent spectra (absorption: λ_{max} = 518, 555, 620 nm; fluorescence: λ_{em} = 573, 670, 730 nm, Figure 4b,d, red lines). These spectral features reflect a significant planarization of the conjugated backbone and interchain aggregation resulting in efficient delocalization of the

(21) (a) Stöber, W.; Fink, A.; Bohn, E. *J. Colloid Interface Sci.* **1968**, *26*, 62–69. (b) Nozawa, K.; Gailhanou, H.; Raison, L.; Panizza, P.; Ushiki, H.; Sellier, E.; Delville, J. P.; Delville, M. H. *Langmuir* **2005**, *21*, 1516–1523.

(22) The GPC trace with M_w = 112000 g/mol cannot correspond to liner P3HT because of solubility arguments: liner P3HTs with M_w > 50000 g/mol are not soluble in THF.

Scheme 3. Schematics Illustrating that at Constant Grafting Density and Chain Length, Chains Grafted to Supporting Particles with Low Surface Curvature Approach Each Other Closely throughout the Whole Chain Length[a]

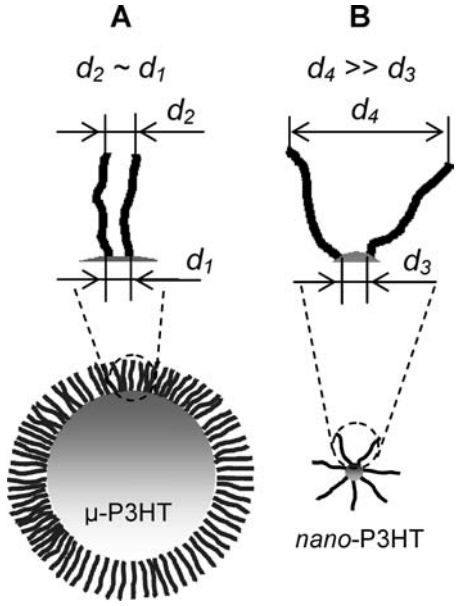

[a] This facilitates chain-stretching and aggregation ($d_2 \sim d_1$, A), whereas at high surface curvature the tethered chains are close to each other close to the grafting points but quickly become separated as one moves away from the grafting point ($d_4 \gg d_3$, B).

π-conjugated electrons (Scheme 3A).[23] It is noteworthy that the shape of the absorption spectra and the position of the absorption maxima remain constant even at very low concentrations of the μ-P3HT particles in THF down to the sensitivity limit of the spectrophotometer, demonstrating that the observed planarization and aggregation of P3HT chains occur at a single-particle level and are not caused by the interparticle aggregation (Figure 4c).[24]

The observed effects can be attributed to the fact that P3HT chains within the densely grafted brush layer are brought closely to each other throughout the whole length ($d_2 \sim d_1$, Scheme 3A) that induces their stretching and facilitates planarization and aggregation even in normally good solvents.

To demonstrate generality of the developed SI-KCTP method, poly(3-dodecylthiophene), P3DDT, was also grafted from 460 nm organosilica particles using the procedure of the preparation of the μ-P3HT particles. SEM measurements reveal that SI-KCTP induces the increase of the particles diameter from 460 up to 515 nm (Figure S10) that corresponds to the shell thickness of about 25 nm (Table 1). The resulting μ-P3DDT particles exhibit optical properties similar to the properties of μ-P3HT. Synthetic and characterization details are given in Supporting Information (Figures S11−13).

To further examine the idea that the optical properties are a function of a macromolecular architecture, the grafting of P3HT from *nanoscale* organosilica particles was performed and the properties of the resulting hairy P3HT nanoparticles were investigated. Due to a high surface curvature of such small-sized particles it is expected that the chain density will decay steeply toward a periphery of the shell ($d_4 \gg d_3$, Scheme 3B), so that even at very high grafting densities (nearby the particle surface) the effects originating from the chain-overcrowding are unlikely here.[25]

Organosilica nanoparticles were obtained via a sol−gel hydrolysis of silane **2** in water-in-oil miniemulsion. After extensive purification from surfactant, the resulting particles were readily soluble in common organic solvents. GPC gave "an apparent" molecular weight of the nanoparticles of about $M_n = 2500$ g/mol against linear polystyrene (PS) standards. Because of a highly compact structure of the nanoparticles and their higher than PS density, the real molar mass of the nanoparticles is assumed to be higher. Dynamic light scattering (DLS) measurements revealed the hydrodynamic radius of the nanoparticles in THF of about 4 nm. Based on these data, we anticipate that each organosilica nanoparticle contains on the order of few tens of residues of the silane **2**.

Grafting of P3HT was performed using the above-described protocol that implies the treatment of the nanoparticles with $Et_2Ni(bipy)$ and dppp followed by addition of **1** at monomer-to-initiator ratio of ∼37/1 (Figures S12−S14). According to TGA, the resulting product, further designated as *nano*-P3HT particles, is P3HT containing 4.3% of noncombustible material, presumably of silica (Figure S12). It has a monomodal GPC trace with $M_n = 35000$ g/mol and $M_w = 75000$ g/mol, as determined by GPC using PS standards or $M_n = 49100$ g/mol and $M_w = 60500$ g/mol, using a light scattering detector. Because of the limited and MW-dependent solubility of P3HT,[26] such a high MW could not be provided by *room temperature* polymerization neither using Ph-Ni(dppp)-Br catalyst (that limits DP) nor with $Ni(dppp)Cl_2$ that does not have end-capping groups. In the grafting experiment, the formation of the high MW P3HT was possible due to a simultaneous growth of a number of P3HT grafts from the multifunctional initiator. A per-graft DP of ∼24 corresponding to $M_n \sim 4000$ g/mol can be deduced from ^{1}H NMR data by integration of main signals and signals from end-groups (Figure S13) that is close to the theoretical per-graft DP value of ∼26 given by the monomer-to-initiator ratio of ∼37/1 and the monomer conversion of ∼70% in this grafting experiment. The hydrodynamic radius determined by DLS of the *nano*-P3HT particles in THF of about 8.5 nm corresponds to the length of 24 thiophene repeat units that fits NMR data (Figure S13). Division of the overall DP of the *nano*-P3HT particles equal to ∼296 (49100/166) on the pregraft DP of 24 gives an approximate number-averaged amount of the P3HT chains attached to the organosilica core of ∼12. The *nano*-P3HT particles exhibit good film-forming properties and an excellent solubility in THF of up to 25−30 g/L at room temperature without signs of aggregation, for example, gelation, precipitation, or change of color (native P3HT is orange in solution when fully dissolved). The aggregation of the *nano*-P3HT particles in THF and xylene was compared with those for linear P3HT samples with different molecular weights.[27] It was found that the *nano*-P3HT particles are much less prone to aggregation when compared to linear P3HT of much lower MW

(23) Magnani, L.; Rumbles, G. I. D.; Samuel, W.; Murray, K.; Moratti, S. C.; Holmes, A. B.; Friend, R. H. *Synth. Met.* **1997**, *84*, 899–900.
(24) Brustolin, F.; Goldoni, F.; Meijer, E. W.; Sommerdijk, N. A. J. M. *Macromolecules* **2002**, *35*, 1054–1059. Kiriy, N.; Jähne, E.; Adler, H.-J.; Schneider, M.; Kiriy, A.; Gorodyska, G.; Minko, S.; Jehnichen, D.; Simon, P.; Fokin, A. A.; Stamm, M. *Nano Lett.* **2003**, *3*, 707–712.
(25) Voudouris, P.; Choi, J.; Dong, H.; Bockstaller, M. R.; Matyjaszewski, K.; Fytas, G. *Macromolecules* **2009**, *42*, 2721–2728.
(26) Zen, A.; Pflaum, J.; Hirschmann, S.; Zhuang, W.; Jaiser, F.; Asawapirom, U.; Rabe, J. P.; Scherf, U.; Neher, D. *Adv. Funct. Mater.* **2004**, *14*, 757–764.
(27) Koppe, M.; Brabec, C. J.; Heiml, S.; Schausberger, A.; Duffy, W.; Heeney, M.; McCulloch, I. *Macromolecules* **2009**, *42*, 4661–4666.

(as determined by GPC) of $M_n = 8000$ and $M_w = 13300$ g/mol. The aggregation behavior and solubility of the *nano*-P3HT particles are very similar to those of linear P3HT with $M_n = 6600$ and $M_w = 8800$ g/mol, that is, to the properties of the sample whose DP approaches the per-graft DP of the *nano*-P3HT particles. A much higher solubility of the *nano*-P3HT particles than that of linear P3HT samples corroborates with a branched nature of the prepared product. It might be tentatively concluded that in contrast to linear P3HTs, the overall MW for branched P3HTs samples is a much less important factor for determining the aggregation behavior, but the contour length of the grafts and the diameter of the *nano*-P3HT particles are crucial parameters here.

The optical properties of the *nano*-P3HT particles in THF and chloroform solutions are very similar to ones for linear untethered P3HT (not shown). This reflects that no overcrowding effects (similar to ones observed in the μ-P3HT particles, Scheme 3A) occur if P3HT chains are attached to the core of a very high surface curvature (Scheme 3B). The absorption of a thermally annealed (150 °C, 5 min) film of the *nano*-P3HT particles is significantly blue-shifted and less intense compared to the absorption of the film with the same thickness made from linear P3HT sample with $M_n = 8000$ and $M_w = 13300$ g/mol (*nano*-P3HT particles, black line in Figure 4e: $\lambda_{max} = 517$ nm, shoulders at 550 and 598 nm; linear P3HT, red line in Figure 4e: $\lambda_{max} = 554$ nm, a shoulder at 602 nm). Such spectral characteristics can be ascribed either to low regioregularitiy (both the shape of the spectrum and the position of the peak are remarkably similar to that for earlier reported P3HT with a low, 86% regioregularity),[28] or to relatively low DP of P3HT. Because ^{1}H NMR reveals rather high HT regioregularity of 97% for the *nano*-P3HT particles (Figure S13), the former explanation can be declined. Thus, we suggest that the prepared product is, in fact, a star-like polymer in which few tens of highly regioregular P3HT arms with an average per-graft DP of ~24 emanate from the cross-linked organosilica core.

Photovoltaic Properties of the *nano*-P3HT Particles. A significant dependence of photovoltaic (PV) performance on both regioregularity[28] of P3HT and on its MW[29] was previously reported, however, the influence of the architecture of P3HTs was not investigated. In the present work we did not intend to establish a comprehensive architecture−property relationship but rather aimed at verifying whether the architecture of P3HT is also a factor able to affect the PV performance. Another motivation to test the PV properties of the *nano*-P3HT particles was to determine if the inclusion of the silica nanoparticles and the preparative procedure had any adverse effects on PV performance. The *nano*-P3HT particles in a combination with PCBM showed a reasonably good PV performance for relatively large area devices with an active area of 1 cm^2 (PCE = 1.8−2.3%, $I_{sc} = 5.5$−6.8 mA cm^{-2}; $V_{oc} = 0.60$−0.62 V; FF = 55−58%; Figure 5 and S14).

Although the PV performance of the *nano*-P3HT particles is lower than for the best reported P3HT-PCBM devices, the observed performance for the *nano*-P3HT particles when employed in a bulk heterojunction with PCBM is similar to what is obtained with linear P3HT with a rather high molecular weight

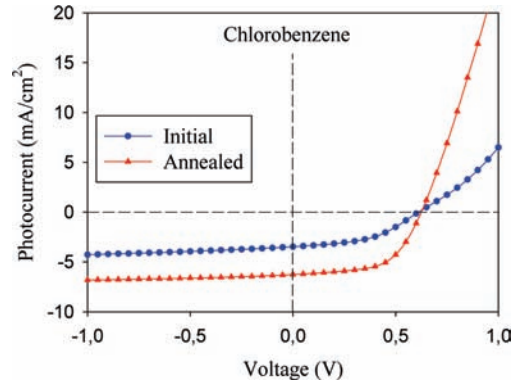

Figure 5. IV curves of Glass/ITO/PEDOT/PSS/*nano*-P3HT particles/PCBM/Al device before (blue circles) and after (red triangle) thermal annealing (130 °C for 5 min).

($M_w = 36\,600$ g/mol) for relatively large active area devices of 1 cm^2.[30] On the other hand, it is even somewhat better than the performance of previously reported small-area devices that utilized relatively low molecular weight P3HTs of $M_w < 13000$ g/mol.[20,29] This result demonstrates that the developed SI-KCTP procedure, at least, does not affect the optoelectronic properties of P3ATs. Although more studies are necessary to comprehensively establish the influence of the polymer architecture on the PV performance, it becomes clear that the molecular weight of linear P3HT constituents of branched P3HT structures must be subjected to further optimization in order to enhance the PV performance.

The fact that at this point we did not obtain clear-cut benefits in PV performance with the *nano*-P3HT particles compared to the benchmark P3HT/PCBM-based devices is not forcibly disappointing because the P3HT/PCBM-based devices are already largely optimized with their performance approaching the theoretical limit for this particular blend. We, therefore, believe that a possible impact of the covalent preorganization would be much more pronounced with systems that exhibit much less self-organization propensity into desired ordered ensembles, such as low bandgap polymers.[1] On the other hand, the particles synthesized in this work (i.e., having the submicrometer or nanometer cores) are obviously not optimal in their size. The larger of them being too large to exhibit acceptable film-forming properties and the smaller ones being too small to show properties substantially deviating from the properties of conventional linear P3HT. From these considerations, the hairy particles with the core size of 20−50 nm would be more attractive for PV applications and they will be a target for further research. Third, we strongly believe that the SI-KCTP strategy presented herein will be applicable for preparation of much more complex and otherwise inaccessible systems comprising, for example, several kinds of conjugated polymers grown from the core. We envisage possibilities for tuning of light-adsorption, charge-transport, or self-assembly properties of the hairy particles using our approach: (i) by a variation of the core nature, size, and shape; (ii) via involvement of other monomers in SI-KCTP to form random, gradient, block copolymer or mixed polymer shells; and (iii) by a proper chain-termination for positioning of additional functionality (e.g., dyes or binding groups) into the periphery of the nanoparticle shell. Recent reports on the preparation of various all-conjugated block

(28) Woo, C. H.; Thompson, B. C.; Kim, B. J.; Toney, M.; Fréchet, J. M. J. *J. Am. Chem. Soc.* **2008**, *130*, 16324–16329.
(29) (a) Schilinsky, P.; Asawapirom, U.; Scherf, U.; Biele, M.; Brabec, C. J. *Chem. Mater.* **2005**, *17*, 2175–2180. (b) Ma, W.; Kim, J. Y.; Lee, K.; Heeger, A. J. *Macromol. Rapid Commun.* **2007**, *28*, 1776–1780.
(30) Krebs, F. C.; Gevorgyan, S. A.; Alstrup, J. *J. Mater. Chem.* **2009**, *19*, 3899–3908.

copolymers via a chain-extension strategy[31] and advanced procedures for selective end-functionalization of polythiophenes[32] complement our SI-KCTP process well and makes the above-listed tasks a valiant cause.

Conclusions

We demonstrated a new strategy for the preparation of (nano)structured conjugated polymer hybrids, that in this work was exemplified by the synthesis of hairy poly(3-alkylthiophene) particles. In particular, poly(3-alkylthiophenes) were selectively grown via a quasi-living surface-initiated Kumada catalyst-transfer polycondensation (SI-KCTP) reaction from particles bearing surface-immobilized Ni catalysts supported by bidentate phosphorus ligands. This resulted in hairy particles with end-tethered P3HT chains. Densely grafted P3HT within the μ-P3HT particles exhibits strongly altered optical properties as compared to the untethered counterparts or to P3HT grafted onto small nanoparticles with a high surface curvature. We attribute this to strong interchain interactions within the densely grafted P3HT chains, which can be tuned by changing of the surface curvature (or size) of the supporting particle. The hairy P3HT nanoparticles were successfully applied in bulk heterojunction solar cells. We believe that the developed SI-KCTP approach can be extended for the preparation of much more complex materials in which many kinds of functional constituents are covalently preorganized.

Acknowledgment. The authors acknowledge the financial support of the Leibniz-Institut für Polymerforschung Dresden e.V. and the Deutsche Forschungsgemeinschaft (KI-1094/3-1). This work was further supported by the Danish Strategic Research Council (DSF 2104-05-0052 and 2104-07-0022) and by EUDP (j. nr. 64009-0050). The authors acknowledge Petra Treppe and Albena Lederer for making GPC measurements.

Supporting Information Available: Materials and equipment data; experimental procedures: synthesis of Ph-Ni(bipy)-Br, Ph-Ni(dppp)-Br, and Ph-Ni(dppe)-Br; model experiments of externally initiated KCTPs; synthesis of organosilane particles; preparation of μ-P3HT, μ-P3DDT, and *nano*-P3HT particles; characterization data of obtained products: NMR, UV−vis, fluorescence spectra, TGA, GPC data; preparation and characterization of solar cell. This material is available free of charge via the Internet at http://pubs.acs.org.

JA904885W

(31) Yokoyama, A.; Kato, A.; Miyakoshi, R.; Yokozawa, T. *Macromolecules* **2008**, *41*, 7271–7273. (a) Miyakoshi, R.; Yokoyama, A.; Yokozawa, T. *Chem. Lett.* **2008**, *37*, 1022–1023.

(32) Liu, J.; McCullough, R. D. *Macromolecules* **2002**, *35*, 9882–9889.